Elastic and nonlinear acoustic properties of $YBa_2Cu_3O_{7-x}$ ceramics with different oxygen contents

Q. Wang, G. A. Saunders, and D. P. Almond
Schools of Physics and Material Science, University of Bath, Claverton Down, Bath BA2 7AY, United Kingdom

M. Cankurtaran
Hacettepe University, Department of Physics, Beytepe, 06532 Ankara, Turkey

K. C. Goretta
Energy Technology Division, Argonne National Laboratory, Argonne, Illinois 60439
(Received 21 November 1994; revised manuscript received 3 April 1995)

The effects of temperature and hydrostatic pressure on the velocities of longitudinal and shear ultrasonic waves propagated in ceramic samples of $YBa_2Cu_3O_{6.3}$, $YBa_2Cu_3O_{6.6}$, and $YBa_2Cu_3O_{6.94}$ have been measured, to examine the effects of oxygen content and ordering on the elastic and nonlinear acoustic properties of $YBa_2Cu_3O_{7-x}$. Corrections have been made by several methods for the effects of sample porosity and microcracking on the elastic properties. Temperature and pressure dependence of the ultrasonic characteristics are compared. The elastic moduli of $YBa_2Cu_3O_{6.3}$ and $YBa_2Cu_3O_{6.94}$ show normal behavior with temperature in accord with a phenomenological model of vibrational anharmonicity down to 40 and 100 K, respectively. Particularly marked elastic stiffening has been found in the temperature dependence of the elastic moduli of $YBa_2Cu_3O_{6.6}$ with decreasing temperature from 270 to 200 K. It is suggested that the origin of this distinctive feature is a relaxation process of oxygen-atom hopping and formation of localized orthorhombic I phase within this orthorhombic II compound. The pressure derivatives of the natural velocities and bulk modulus of $YBa_2Cu_3O_{6.3}$, $YBa_2Cu_3O_{6.6}$, and $YBa_2Cu_3O_{6.94}$ tend to decrease with increasing oxygen content. Using the results obtained in this work and some data published previously, we have shown that the pressure derivative $(\partial B^s/\partial P)_{P=0}$ of the adiabatic bulk modulus of $YBa_2Cu_3O_{7-x}$ is correlated strongly with sample porosity and decreases approximately linearly with decreasing n/P_m, the ratio of porosity n to the maximum applied pressure P_m. We have also shown that values of the mean acoustic mode Grüneisen parameter γ^{el} of ceramic superconducting compounds, determined by ultrasonic measurements, have a linear relationship with the porosity n. The effects of oxygen contents on the pressure derivative $(\partial B^S/\partial P)_{P=0}$ of $YBa_2Cu_3O_{7-x}$ are also discussed.

I. INTRODUCTION

The superconducting and other physical properties of $YBa_2Cu_3O_{7-x}$ are extremely sensitive to composition, in particular, oxygen content. The ultrasonic velocities and the elastic stiffnesses of $YBa_2Cu_3O_{7-x}$ depend on the oxygen content but information in detail of the effects is sparse, indeterminate, and contradictory. Kim *et al.*[1] reported that the values of both longitudinal and shear velocities (and hence that of the bulk modulus) at 220 K decrease with increasing oxygen content from 6.2 to 6.9. Hikata *et al.*[2] found that at low temperatures ($T \leq 1$ K), the value of the transverse wave velocity increases as the oxygen content is increased from $O_{6.42}$ to O_7. A sharp decrease in the values of Poisson's ratio and bulk modulus of ceramic $YBa_2Cu_3O_{7-x}$ as the oxygen content is increased beyond 6.4 was reported by Lemmens *et al.*[3] at 2.4 K. In a collation of the room-temperature elastic constants for eleven polycrystalline $YBa_2Cu_3O_{7-x}$ samples with oxygen contents from 6.2 to 6.9, Ledbetter[4] noted a lack of systematic dependence on oxygen content. Hence, further study is needed to clarify the question: How do the elastic properties of polycrystalline $YBa_2Cu_3O_{7-x}$ depend on oxygen content? In this work the temperature and hydrostatic pressure dependences of the elastic properties of polycrystalline $YBa_2Cu_3O_{7-x}$ have been measured on three high-quality ceramic samples of differing oxygen content: $YBa_2Cu_3O_{6.3}$, $YBa_2Cu_3O_{6.6}$, and $YBa_2Cu_3O_{6.94}$. The data obtained provide some useful clarification of the effects of oxygen content, porosity, and cracking on the elastic moduli and their pressure derivatives.

II. EXPERIMENTAL PROCEDURES

Phase-pure $YBa_2Cu_3O_{7-x}$ powder was synthesized from Y_2O_3, $BaCO_3$, and Cu-O by solid-state reaction in flowing oxygen at reduced pressure.[5] The powder was ground in a tungsten carbide rotary mill and then cold pressed at 140 MPa in a cylindrical die 12.7 mm in diameter. The pellets were placed on Mg-O single crystals and sintered for 4 h at 935 °C in dry, CO_2-free air. Oxygen contents were established as follows:[6] 6.94, set by annealing for 14 h at 425 °C in oxygen; 6.6, set by annealing for 16 h at 521 °C in 0.1% oxygen/balance Ar; and 6.3, set by annealing for 16 h at 648 °C in 0.1% oxygen/balance Ar.

To fix the oxygen content, but avoid microcracking, two cooling schedules were followed. The pellet heated at 425 °C in oxygen was quickly moved to a part of the furnace that was at 250 °C, held for a few minutes, and then cooled at ≈3 °C/min to room temperature. The pellets heated in 0.1% oxygen were cooled to room temperature at 3 °C/min. During cooling, a vacuum was slowly drawn so that the oxidizing potential of the atmosphere remained approximately constant.[6,7] The density of the samples was measured by applying Archimedes' principle, and the porosity (n) was evaluated by comparing measured density with theoretical x-ray density. The results of a scanning electron microscopy study show that the grain size in the three samples was between 5 and 10 μm.

The pellets were polished to have flat and parallel faces to $\approx 10^{-4}$ rad. Ultrasonic pulses were generated and detected by X- and Y-cut (for longitudinal and shear waves, respectively) 5–10 MHz quartz transducers. The temperature dependences of ultrasonic wave velocity and attenuation were measured in a closed cycle refrigerator in the temperature range of 10 to 300 K, with transducers bonded to the specimens using Nonaq. Hydrostatic pressures up to 0.16 GPa were applied at room temperature with a piston-and-cylinder apparatus with silicone oil as the pressure-transmitting medium and Dow resin as the transducer-bonding material. Pressure was measured with a calibrated manganin resistance gauge. To determine the effects of temperature and pressure on the ultrasonic wave transit time, a pulse-echo overlap system[8] capable of measuring changes to better than 1 part in 10^5 in ultrasonic transit time was used. A transducer correction[9] was applied to the ultrasonic wave velocities. The "natural velocity (W)" technique[10] was used to sidestep the effects of pressure-induced changes in sample dimensions.

III. EFFECTS OF POROSITY, OXYGEN CONTENT, AND TEMPERATURE ON THE ULTRASONIC VELOCITIES AND ELASTIC PROPERTIES

In order to check the anisotropy of the samples, ultrasonic waves were propagated both parallel and perpendicular to the pressing direction. There was no significant difference in ultrasonic wave velocities propagated in different directions: the values of the wave velocities of the longitudinal and shear modes propagated along the direction perpendicular to the pressing direction were only about 3% and 2.4% larger than those of the waves propagated along the pressing direction. Within the limits of experimental error, the anisotropy caused by the intrinsic properties of the materials can be taken to be insignificant. Hence, this work was concentrated on the measurements of the wave modes propagated along the pressing direction. These particular $YBa_2Cu_3O_{7-x}$ ceramics can be treated as isotropic materials with two independent elastic moduli C_L (longitudinal modulus) and μ (shear modulus), because the grain size in the samples is much smaller than the ultrasonic wavelength (e.g., for a 10 MHz longitudinal ultrasonic wave traveling with a velocity about 4500 ms^{-1}, the wavelength is 450 μm, which is much greater than the grain size of the samples). The bulk modulus B^S, Young's modulus E, Poisson's ratio σ, and the elastic Debye temperature Θ_D^{el} have been determined by using the measured sample density and velocities of longitudinal and shear ultrasonic waves propagated in the specimens. Limited data for $YBa_2Cu_3O_{6.94}$ have been reported previously in a short communication.[11] Table I collects the results at 295 K for $YBa_2Cu_3O_{6.3}$, $YBa_2Cu_3O_{6.6}$, and $YBa_2Cu_3O_{6.94}$.

A. Comparison between methods for correction for effects of porosity and microcracking on elastic properties of $YBa_2Cu_3O_{7-x}$ ceramic samples

In a ceramic high-T_c material, both pores and cracks are introduced during the fabrication process. The pores and cracks in a sample have a strong influence on its density and the values of the elastic moduli. The densities of high-T_c ceramics generally fall in a range from 50 to 95% of the theoretical density. To compare the elastic properties of $YBa_2Cu_3O_{7-x}$ ceramic samples with differing oxygen content and to investigate their intrinsic properties, it is necessary to correct for the effects of porosity and microcracking on the measured (or effective)

TABLE I. Porosity, ultrasonic wave velocities, and elastic moduli at 295 K and the Debye temperature [calculated from data obtained at 10 K (*) or 15 K (**)]. Data are given for both sintered ceramic samples and corresponding void-free matrices.

	$YBa_2Cu_3O_{6.3}$		$YBa_2Cu_3O_{6.6}$		$YBa_2Cu_3O_{6.94}$	
Variable	Ceramic	Void-free	Ceramic	Void-free	Ceramic	Void-free
Porosity n	0.13		0.15		0.12	
Density ρ ($kg\,m^{-3}$)	5470	6278	5365	6323	5560	6338
V_L ($m\,s^{-1}$)	3740	4083	4570	5060	4657	5105
V_S ($m\,s^{-1}$)	2200	2380	2730	3002	2590	2772
C_L (GPa)	76.6	104.8	112.0	161.6	120.6	164.7
μ (GPa)	26.4	35.6	40.1	56.9	37.3	48.6
B^S (GPa)	41.4	57.4	58.5	85.8	70.8	99.9
E (GPa)	65.3	88.5	97.9	140.0	95.2	125.5
σ	0.237	0.243	0.221	0.228	0.276	0.291
Θ_D^{el} (K)	294*	334*	374*	434*	356**	400**

moduli.

The correction methods commonly used are those developed for porous or cracked bodies, such as ceramics and rocks, or those for a composite with inclusions. Different methods based on distinct approaches that restrictively account for one or a few factors (porosity, dimensions, and shape of the cracks, etc.) can give different values for the corrected elastic moduli. A comparison needs to be made between the corrected values obtained for the elastic moduli to examine the influence of a particular correction method. Sayers and Smith[12] extended a self-consistent treatment to the problem of porous materials with porosity up to 30%, based on a multiple-scattering theory developed by Lloyd and Berry[13] for propagation of waves through a random assembly of spheres. With their method, Sayers and Smith[12] could obtain the longitudinal and shear mode velocities of ultrasonic waves propagated in a matrix; only the effects of the porosity of the sample were considered. Cankurtaran *et al.*[14] developed equations to calculate the bulk and shear moduli of the matrix with a theoretical treatment of the wave propagation under pressure in an isotropic solid in which the distribution of pores is uniform. Both the porosity and the bulk modulus of the pore-filling fluid are included in this method of correction. If the specimen is at atmospheric pressure in air or under vacuum, the porosity is the only factor effective in this model. Ledbetter *et al.*[15] used a model considering only the effects of the porosity for particle-reinforced composites,[16] assuming that the voids (pores) are spherical and randomly distributed. Budiansky and O'Connell[17] calculated the elastic moduli of solids containing randomly distributed flat cracks on the basis of the self-consistent treatment on potential-energy changes in cracked solids. Their method considers the shape and size of the cracks and the number of cracks per unit volume.

The corrected values of ultrasonic wave velocities and elastic moduli for the nonporous (void-free) matrices of $YBa_2Cu_3O_{6.3}$, $YBa_2Cu_3O_{6.6}$, and $YBa_2Cu_3O_{6.94}$, obtained by using each of these four methods, are presented in Table II. The results corrected by using the wave-scattering[12] (WST) and wave-propagation[14] (WPT) theories agree well with each other. The model for particle-reinforced composites[15] (PRC) gives similar results but produces values for velocities and elastic moduli lower than those of the above two methods. The results found from the theory of potential-energy change[17] (PEC) depend on the shape and the average dimensions of the cracks. To expedite this last method, three models for the crack shape have been assumed for $YBa_2Cu_3O_{6.3}$ and $YBa_2Cu_3O_{6.94}$ samples: (a) circular cracks with average radius $r_a=4.0$ μm and thickness $r_c=0.74$ μm, (b) long

TABLE II. Corrected results obtained by using different methods of correction for effects of porosity and cracking on ultrasonic wave velocities V_L and V_S, elastic moduli C_L, μ, and B^S, and Poisson's ratio σ for sintered $YBa_2Cu_3O_{6.3}$, $YBa_2Cu_3O_{6.6}$, and $YBa_2Cu_3O_{6.94}$ at 295 K. Abbreviations are as follows: WST = wave-scattering theory (Ref. 12), WPT = wave-propagation theory (Ref. 14), PRC = particle-reinforced composites (Ref. 15), PEC = theory of potential-energy change (Ref. 17), with (a) circular cracks with average radius $r_a=4.0$ μm and thickness $r_c=0.74$ μm; (b) long thin ellipsoidal cracks with average semiaxes $r_a=4.0$ μm, $r_b=1.0$ μm, and $r_c=0.4$ μm; and (c) long rectangular cracks with average sizes $2r_a=8.0$ μm, $2r_b=2.0$ μm, and $2r_c=0.64$ μm; for $YBa_2Cu_3O_{6.6}$: (a) $r_c=0.79$ μm, (b) $r_c=0.32$ μm, and (c) $2r_c=0.5$ μm; other dimensions are same as above.

Methods	V_L (m/s)	V_S (m/s)	C_L (GPa)	μ (GPa)	B^S (GPa)	σ
			$YBa_2Cu_3O_{6.3}$			
WST	4083	2380	104.8	35.6	57.4	0.243
WPT	4087	2375	105.0	35.5	57.7	0.245
PRC	4000	2330	100.6	34.1	55.1	0.243
PEC (a)	4076	2585	104.5	42.0	48.5	0.164
PEC (b)	4088	2598	105.0	42.4	48.5	0.161
PEC (c)	4080	2590	104.6	42.2	48.4	0.162
			$YBa_2Cu_3O_{6.6}$			
WST	5060	3002	161.6	56.9	85.8	0.228
WPT	5056	3006	161.4	57.1	85.3	0.226
PRC	4915	2928	152.4	54.1	80.3	0.225
PEC (a)	5049	3377	160.6	71.9	64.8	0.095
PEC (b)	5043	3374	160.2	71.7	64.6	0.095
PEC (c)	5045	3378	160.7	72.0	64.6	0.093
			$YBa_2Cu_3O_{6.94}$			
WST	5105	2772	164.7	48.6	99.9	0.291
WPT	5104	2772	164.6	48.6	99.8	0.291
PRC	4998	2729	157.8	47.1	95.1	0.287
PEC (a)	5089	2875	163.6	52.2	94.0	0.265
PEC (b)	5091	2877	163.8	52.3	94.0	0.265
PEC (c)	5082	2871	163.2	52.1	93.7	0.266

thin ellipsoidal cracks with average semiaxes $r_a = 4.0$ μm, $r_b = 1.0$ μm, and $r_c = 0.4$ μm, and (c) long rectangular cracks with average sizes $2r_a = 8.0$ μm, $2r_b = 2.0$ μm, and $2r_c = 0.64$ μm. The average dimensions for the shape of each crack have been chosen to give a longitudinal modulus (C_L) a value close to that obtained by using the wave-scattering[12] and wave-propagation[14] theories. The results of the theory of potential-energy change[17] depend very much on the product of the sample porosity and the aspect ratio of the cracks. The specimen of $YBa_2Cu_3O_{6.6}$ had a porosity (0.15) larger than those of $YBa_2Cu_3O_{6.3}$ (0.13) and $YBa_2Cu_2O_{6.94}$ (0.12). Hence, to treat the $YBa_2Cu_3O_{6.6}$ sample in the PEC model, the crack thickness r_c was chosen to be 0.79 and 0.25 μm for the circular cracks and rectangular cracks, respectively, and 0.32 μm for the semiaxis r_c of the long thin ellipsoidal cracks, the other dimensions being the same as those selected for the $YBa_2Cu_3O_{6.3}$ and $YBa_2Cu_3O_{6.94}$ samples. It can be seen from Table II that this method, as compared with others, gives larger values for shear modulus and shear mode velocity, hence, smaller values for bulk modulus and Poisson's ratio, in particular, for $YBa_2Cu_3O_{6.6}$. Examination of the corrected results (Table II) provided by each of the procedures suggests that the methods of the self-consistent wave-scattering theory and the wave-propagation theory give a concordant correction for the effects of porosity on the ultrasonic data. Therefore, the results of the WST have been taken as those of the void-free compounds in Table I. The PEC model indicates that the values of ultrasonic wave velocities and elastic moduli of ceramic $YBa_2Cu_3O_{7-x}$ may be sensitive to the sample porosity and the aspect ratio of cracks. The results of this model imply that at atmospheric pressure the effects of cracks on wave velocities are slightly larger for shear waves than for longitudinal waves. An analysis made by Shindo, Ledbetter, and Nozaki[18] in a recent paper showed that both the bulk and shear moduli vary slowly near the spherical limit with the void aspect ratio equal to 1, while the moduli vary rapidly near the oblate limit with the void aspect ratio approaching zero. The three methods,[13–15] which take into account only the effects of porosity, give similar results after correction. Comparison of these results (Table II) with the measured data (Table I) indicates that pores affect longitudinal ultrasonic wave velocities slightly more than shear wave velocities. The analysis by Shindo, Ledbetter, and Nozaki[18] shows that voids have more effects on Young's modulus than on the shear modulus. The corrections made by the WST and the WPT methods give the bulk modulus B^S with the values (Table II) close (81% for $YBa_2Cu_3O_{6.94}$ and 77% for $YBa_2Cu_3O_{6.6}$) to those determined by Jorgensen *et al.*[19] for $YBa_2Cu_3O_{6.93}$ (123 GPa) and $YBa_2Cu_3O_{6.6}$ (112 GPa), using neutron powder diffraction under hydrostatic pressure up to 0.6 GPa.

B. Effects of oxygen content and ordering on elastic properties of $YBa_2Cu_3O_{7-x}$

The longitudinal velocity and modulus and the bulk and Young's moduli of $YBa_2Cu_3O_{7-x}$ show a tendency to increase with oxygen content (Table I). By contrast, the values of shear wave velocity and shear modulus of $YBa_2Cu_3O_{6.6}$ are higher than those for $YBa_2Cu_3O_{6.3}$ and $YBa_2Cu_3O_{6.94}$. Because the elastic Debye temperature Θ_D^{el} is more heavily weighted by the shear wave velocity, the value of Θ_D^{el} for $YBa_2Cu_3O_{6.6}$ is also larger than that of $YBa_2Cu_3O_{6.3}$ and $YBa_2Cu_3O_{6.94}$. The systematic increases in the longitudinal velocity and modulus, and in the bulk and Young's moduli for the three $YBa_2Cu_3O_{7-x}$ ceramics would be expected to result from a volume-dependent mechanism. The nonsuperconducting compound $YBa_2Cu_3O_{6.3}$ is in a disordered, tetragonal (T) phase in which the oxygen sites in both the Cu-O_2 plane and the O-Cu-O chain plane are randomly occupied by oxygen ions. Experimental[20] and theoretical studies[21] indicate that the low-transition-temperature, superconducting compound $YBa_2Cu_3O_{6.6}$ is in a phase dominated by the ordered orthorhombic II (ortho-II) structure, in which the oxygen ions tend to occupy every other copper row in the plane that contains the "chains," and hence the phase has a double-cell structure. The superconducting compound $YBa_2Cu_3O_{6.94}$ has the orthorhombic I (ortho-I) phase; the majority of the sites in the chain plane are filled. For reference the crystal structure of $YBa_2Cu_3O_7$ is depicted in Fig. 1; the labels for the atoms follow those used by Santoro.[22] Changes in the ordering of the oxygen ions in $YBa_2Cu_3O_{7-x}$ compounds alter the interionic forces. Removal of an oxygen in $YBa_2Cu_3O_{7-x}$ increases the volume of the compound.[23] There is evidence[22] that removing the oxygen ions in the chain plane causes changes in the bond lengths in $YBa_2Cu_3O_{7-x}$ compounds; the changes in the bond lengths of $YBa_2Cu_3O_{6+\delta}$ compounds with oxygen content δ are plotted in Figs. 2(a)–2(c). As δ decreases from 1 to 0, the bond length Cu(2)-O(1) increases and that of Cu(1)-O(1) decreases dramatically [Figs. 2(a) and 2(b)], while the bond lengths Cu(1)-O(4), Cu(2)-O(2), and Cu(2)-O(3) remain almost constant [Fig. 2(b)]. In the process of disordering, O(4) atoms are gradually removed, a

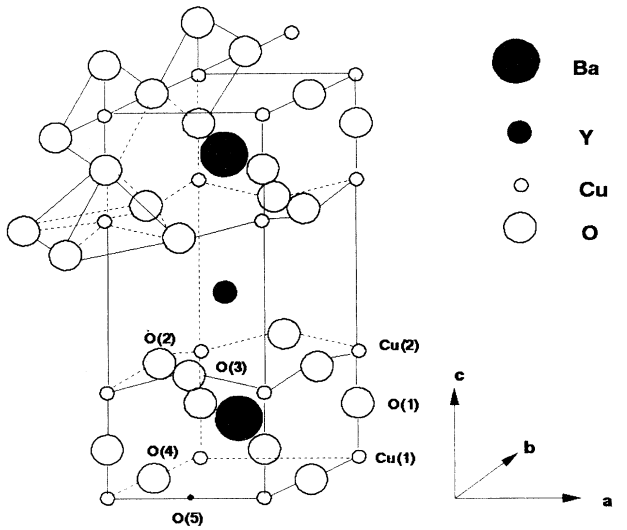

FIG. 1. Crystal structure of $YBa_2Cu_3O_7$. The labels of the atoms are those used by Ref. 22.

process accompanied by the weakening and eventual elimination of the repulsive forces between O(4) and O(1) atoms. The effect is to move the plane of O(1) atoms toward Cu(1) atoms. At the same time, the bond lengths Ba-O(1) and Ba-O(4) increase with reducing δ, while the lengths Ba-O(2) and Ba-O(3) decrease [Fig. 2(c)]. This finding indicates that barium atoms move along the c axis towards the plane of O(2) and O(3) atoms due to the weakening of the attractive forces from the chain plane. In this process the coordination of the barium atoms changes from tenfold to eightfold.[22] The bond lengths Y-O(2) and Y-O(3) do not change significantly [Fig. 2(a)]. Hence, the transition from the ordered to the disordered phase caused by the removal of the O(4) [and O(5)] atoms leads to elongation of the unit cell along the c axis, which has been established by structural studies of $YBa_2Cu_3O_{7-x}$ by Beech *et al.*[24] and Santoro *et al.*[25] The results of their investigations show that the lattice parameter c is 11.6762 Å for $YBa_2Cu_3O_7$ and 11.8194 Å for $YBa_2Cu_3O_{6.07}$. A study of $YBa_2Cu_3O_{6.85}$ by David *et al.*[26] gives $c = 11.6687$ Å. During the transition process, the volume of the unit cell increases from 173.27 Å^3 for $YBa_2Cu_3O_7$ to 175.83 Å^3 for $YBa_2Cu_3O_{6.07}$.[22] Jorgensen *et al.*[27] determined the structural properties of $YBa_2Cu_3O_{7-x}$ with $0.07 < x < 0.91$ by neutron powder diffraction. They found that when the oxygen content $(7-x)$ was decreased from 6.93 and 6.09, the parameter c and the unit-cell volume increased by $\approx 1.2\%$ and 1.5%, respectively; the bond length Cu(1)-O(1) decreased by $\approx 3\%$ while Cu(2)-O(1) increased by $\approx 7.4\%$. The distance Cu(2)-Cu(2) along the c axis also decreased by $\approx 2.7\%$, i.e., the dimensional changes were accompanied

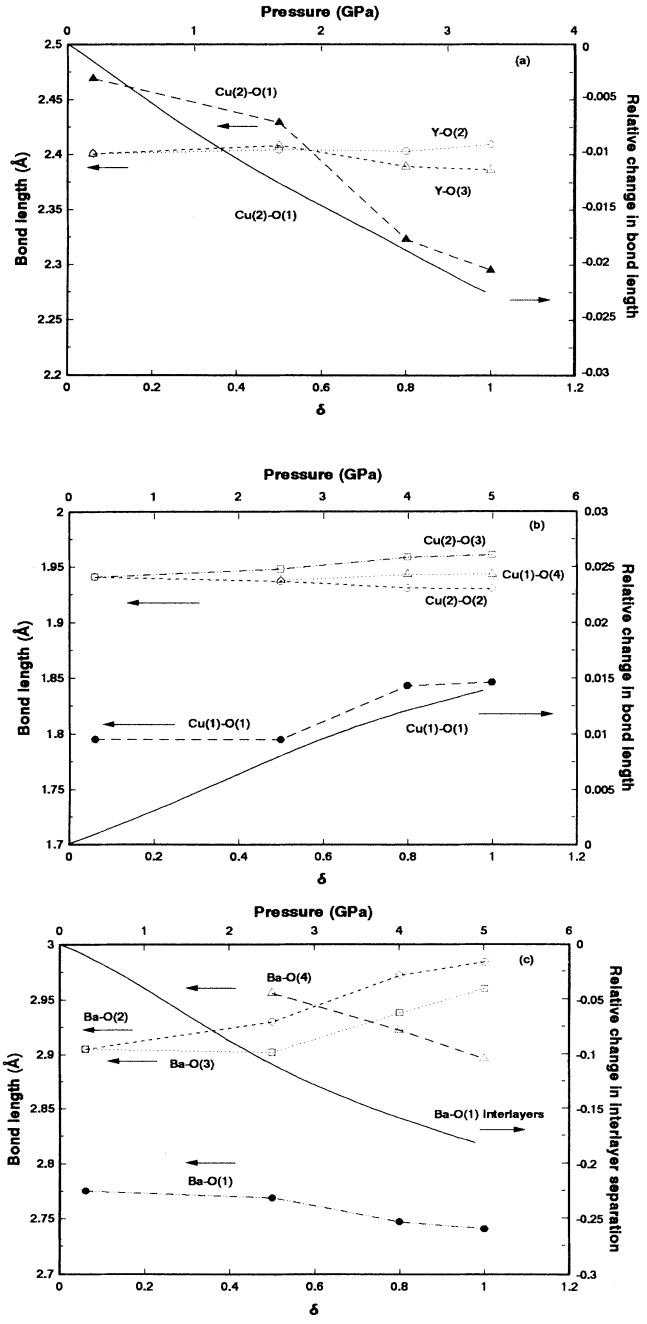

FIG. 2. Bond lengths of $YBa_2Cu_3O_{6+\delta}$ as a function of δ (data taken from Ref. 22). Dotted, dashed, broken, and double-dot-dashed lines are intended solely to guide the eye. The solid lines show the pressure dependence of relative changes in the bond lengths Cu(2)-O(1) and Cu(1)-O(1) and that in the Ba-O(1) interlayer separation calculated by using the data taken from the results of Loveday *et al.* (Ref. 59).

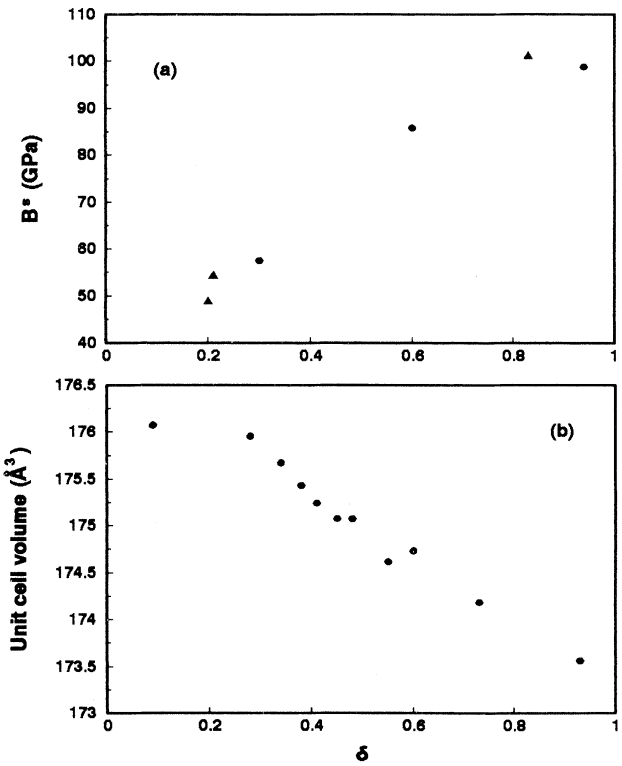

FIG. 3. Oxygen content (δ) dependence of (a) bulk modulus B^S of $YBa_2Cu_3O_{6+\delta}$ ceramic samples (corresponding to void-free matrices); the solid circles correspond to the results of this work and the solid triangles correspond to the data taken from Ref. 4, and (b) unit-cell volume of $YBa_2Cu_3O_{6+\delta}$ (data from Ref. 27).

by the CuO_2 planes approaching each other and by the separation of the chain planes from the CuO_2 planes. These facts suggest that the transitions from the ortho-I to ortho-II, and eventually, to the tetragonal phase are accompanied by weakening of the interionic forces; this would be expected to cause the reduction in the values of ultrasonic velocities and the corresponding elastic moduli found in Table I. The experimental investigations by Drescher-Krasicka[28] of the velocity and attenuation of ultrasonic waves propagated in $YBa_2Cu_3O_{7-x}$ show that the velocity changes with oxygen ordering in the basal Cu-O plane, i.e., the oxygen intake causes an increase in the ultrasonic velocity, whereas the oxygen loss leads to a decrease. It was found that the spatially averaged elastic modulus of a polycrystalline tetragonal sample is 85% of the modulus of the 91 K phase (ortho-I phase) and is 95% of that of the 60 K phase (ortho-II phase). The present results (Table I) are in reasonable agreement with those findings. Using our results for the bulk modulus B^S (after correction for the effects of porosity by the wave-scattering theory) of samples with $\delta=0.3$, 0.6, and 0.94 and those of Ledbetter[4] for the void-free state of the samples with $\delta=0.2$, 0.21, and 0.83, we have found an approximately linear dependence of the bulk modulus B^S on δ [Fig. 3(a)]. For comparison, the unit-cell volume determined by Jorgensen *et al.*[27] is plotted in Fig. 3(b) as a function of δ. The decrease in the bulk modulus is clearly correlated with the increase in the unit-cell volume as the oxygen content is decreased.

C. Temperature dependences of the ultrasonic wave velocities and elastic moduli

The temperature dependences of the longitudinal and shear velocities measured for $YBa_2Cu_3O_{6.3}$, $YBa_2Cu_3O_{6.6}$, and $YBa_2Cu_3O_{6.94}$ are plotted in Figs. 4(a)–4(b). The velocities increase smoothly with decreasing temperature and show no measurable effects near the superconducting transition temperature T_c for $YBa_2Cu_3O_{6.6}$ and $YBa_2Cu_3O_{6.94}$ within the limits of experimental resolution (10^{-5} in changes in ultrasonic wave velocities). A small discontinuity with $\Delta v/v \approx 3-5\times10^{-5}$ of the sound velocity of the longitudinal mode along the c axis was observed at T_c for single-crystal samples of $YBa_2Cu_3O_{7-x}$ by Golding *et al.*[29] and Saint-Paul *et al.*[30] This small discontinuity in the longitudinal mode wave velocity is expected to be smeared out in polycrystalline samples. The anomalous elastic effects and pronounced thermal hysteresis observed by several groups in various $YBa_2Cu_3O_{7-x}$ superconductors in the temperature range 190–240 K have not been found either in the tetragonal $YBa_2Cu_3O_{6.3}$ or in the fully oxygenated orthorhombic $YBa_2Cu_3O_{6.94}$ ceramics. However, the behaviors of both longitudinal and shear mode velocities with temperature are different for the three compounds. The velocities of the ultrasonic waves propagated in $YBa_2Cu_3O_{6.3}$ have the lowest rate of increase with decreasing temperature, whereas those for $YBa_2Cu_3O_{6.6}$ have the highest. The most distinctive difference is that the velocities of the ultrasonic waves propagated in $YBa_2Cu_3O_{6.6}$ increase sharply with decreasing temperature from 270 to 200 K. We now turn to consider this.

Table III compares the temperature derivatives of the ultrasonic wave velocities and those of the elastic moduli C_L, μ, and B^S between 200 and 270 K, which have been obtained by a linear fit to the experimental data in this temperature range, for the three $YBa_2Cu_3O_{7-x}$ compounds with different oxygen contents. All of the temperature derivatives are largest for $YBa_2Cu_3O_{6.6}$ and smallest for $YBa_2Cu_3O_{6.3}$. The temperature dependences of the bulk modulus B^S, Young's modulus E, and Poisson's ratio σ determined from the measurements made on $YBa_2Cu_3O_{6.3}$, $YBa_2Cu_3O_{6.6}$, and $YBa_2Cu_3O_{6.94}$ are compared in Figs. 5(a)–5(c). The temperature dependences of the bulk and Young's moduli for $YBa_2Cu_3O_{6.3}$ and $YBa_2Cu_3O_{6.94}$ show normal behavior without any marked anomalies. However, there is a sharp increase in the temperature dependences of the velocities of both longitudinal and shear modes [Figs. 4(a) and 4(b)] and Young's modulus [Fig. 5(b), middle panel] of $YBa_2Cu_3O_{6.6}$ in the range from 270 to 200 K. In contrast, the increase in B^S of this compound with temperature is not as sharp as that of the other moduli [Fig. 5(a), middle panel], although the increase of B^S is also the highest in this temperature range among the three compounds. This finding indicates that the observed

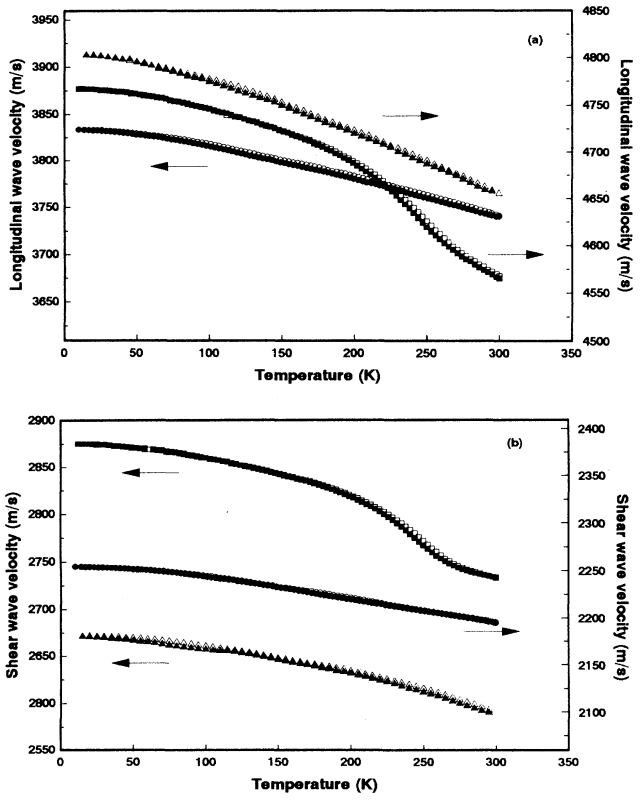

FIG. 4. Temperature dependence of the velocities of (a) longitudinal and (b) shear ultrasonic waves propagated in ceramic specimens of $YBa_2Cu_3O_{6.3}$ (circles), $YBa_2Cu_3O_{6.6}$ (squares), and $YBa_2Cu_3O_{6.94}$ (triangles). The solid (open) symbols correspond to data obtained during cooling (warming).

TABLE III. Temperature derivatives of the ultrasonic wave velocities V_L and V_S and of the elastic moduli C_L, μ, and B^S for $YBa_2Cu_3O_{6.3}$, $YBa_2Cu_3O_{6.6}$, and $YBa_2Cu_3O_{6.94}$ between 200 and 270 K.

Compounds	$(\partial V_L/\partial T)_P$ ($m\,s^{-1}\,K^{-1}$)	$(\partial V_S/\partial T)_P$ ($m\,s^{-1}\,K^{-1}$)	$(\partial C_L/\partial T)_P$ (10^{-7} Pa K^{-1})	$(\partial \mu/\partial T)_P$ (10^{-7} Pa K^{-1})	$(\partial B^S/\partial T)_P$ (10^{-7} Pa K^{-1})
$YBa_2Cu_3O_{6.3}$	−0.40	−0.25	−1.66	−0.61	−0.55
$YBa_2Cu_3O_{6.6}$	−1.38	−1.07	−6.89	−3.20	−2.28
$YBa_2Cu_3O_{6.94}$	−0.66	−0.40	−3.47	−1.17	−1.16

stiffening in the ultrasound velocities of $YBa_2Cu_3O_{6.6}$ in the range from 270 to 200 K involves a rather larger component of shear than volume instability. The value of Poisson's ratio of the three compounds are within the range of values found for perovskite-structure oxides. A broad maximum is found in Poisson's ratio of $YBa_2Cu_3O_{6.6}$ at $\approx$270 K, which may be related to the elastic stiffening observed in the same temperature range, accompanied by a fast decrease down to 200 K; in the range below 200 K, σ is almost independent of temperature. The values of Poisson's ratio for $YBa_2Cu_3O_{6.3}$ and $YBa_2Cu_3O_{6.94}$ are almost constant over the whole temperature range [Fig. 5(c)].

In the absence of instability due to an incipient phase change, the increase in ultrasonic velocities and elastic moduli with decreasing temperature is a consequence of the vibrational anharmonicity. Assuming a phenomenological model, Lakkad[31] has shown that, when the anharmonicity of atomic oscillators is considered, the temperature dependence of the elastic modulus M can be described by the equation

$$M = M_0\left[1 - KF\left[\frac{T}{\Theta_D}\right]\right], \tag{1}$$

where M_0 and K are constants and Θ_D is the Debye temperature. The constant K is related to the ratio of the anharmonic part to the harmonic part of restoring force constants, and M_0 corresponds to the elastic modulus at 0 K. The Debye function $F(T/\Theta_D)$, which describes the anharmonic nature of the vibrations, is given by

$$F\left[\frac{T}{\Theta_D}\right] = 3\left[\frac{T}{\Theta_D}\right]^4 \int_0^{\Theta_D/T} \frac{x^3}{e^x - 1}\,dx\ . \tag{2}$$

Equation (1) has been fitted to the temperature dependences of the longitudinal wave velocities (corrected for the effects of porosity by using the wave-scattering theory) of $YBa_2Cu_3O_{6.3}$, $YBa_2Cu_3O_{6.6}$, and $YBa_2Cu_3O_{6.94}$, taking the values given in Table I for the elastic Debye temperature Θ_D^{el} of the void-free matrices of these ceramics. The results are plotted in Figs. 6(a)–6(c), together with the attenuation data. It can be seen that Eq. (1) fits well to the data sets for $YBa_2Cu_3O_{6.3}$ and $YBa_2Cu_3O_{6.94}$ down to $\approx$40 and 100 K, respectively, while it fits to the data for $YBa_2Cu_3O_{6.6}$ only in the temperature regions of 300–250 and 100–50 K. The velocities of ultrasonic waves propagated in the ortho-II compound $YBa_2Cu_3O_{6.6}$ rise quickly with decreasing temperature below 250 K and then show behavior similar to that of the other two polycrystalline compounds in the range $T < 100$ K. The deviation of the velocity versus temperature curve for $YBa_2Cu_3O_{6.6}$ from the anharmonic prediction is associated with an attenuation peak centered at $\approx$250 K [see Fig. 6(b)], which is absent for $YBa_2Cu_3O_{6.3}$ and $YBa_2Cu_3O_{6.94}$ ceramics. An attenuation peak, or related hysteresis in the ultrasonic wave velocity, at $\approx$230–250 K in sintered polycrystalline $YBa_2Cu_3O_{7-x}$, has been reported by many authors (see for instance, Refs. 32–36) and has been attributed to (i) a phase transformation due to reordering of oxygen atoms in the Cu-O basal planes forming a second phase[34] and (ii) the structural defects, i.e., twins or dislocations.[37] Investigation of the phase diagram of $YBa_2Cu_3O_{7-x}$ has shown that no crystal-structure-related phase transformation occurs below 300 K for the phases with $(7-x)=6.94$ and 6.6. The attenuation peak observed in the sintered $YBa_2Cu_3O_{6.6}$ ceramic sample can hardly be attributed to twinning effects because it is absent in the data for $YBa_2Cu_3O_{6.94}$, which is also twinned. A conceivable reason for this attenuation peak and the related enhancement of the increment of the ultrasonic wave velocity could be hopping of oxygen atoms, which is a thermally activated process.[38] In $YBa_2Cu_3O_{6.6}$, each Cu-O chain is neighbored by two oxygen-missing Cu-□ chains (where □ indicates the vacant oxygen sites) (see Ref. 21). It can be

TABLE IV. Hydrostatic pressure derivatives, at room temperature, of the elastic moduli and natural wave velocities of (1) $YBa_2Cu_3O_{6.3}$, (2) $YBa_2Cu_3O_{6.6}$, (3) $YBa_2Cu_3O_{6.94}$ (this work), (4) hot-pressed $YBa_2Cu_3O_{7-x}$ with $T_c=60$ K (Ref. 40), and (5) $YBa_2Cu_3O_{7-x}$, those extrapolated from ultrasonic measurements on $YBa_2Cu_3O_{7-x}$/Ag composites (Ref. 41), and the mean acoustic-mode Grüneisen parameters for (1), (2), and (3). n and x are porosity and oxygen deficiency of samples and P_m is the maximum pressure applied in measurements. The hydrostatic pressure derivatives of the parameters in (4) are for $P=1$–3 GPa. * denotes values estimated from published data.

	(1)	(2)	(3)	(4)	(5)
ρ ($kg\,m^{-3}$)	4544	5365	5560	5960	5989*
P_m (GPa)	0.16	0.16	0.15	3.0	0.5
n	0.28	0.15	0.12	0.06	0.055
x	0.7	0.4	0.06	0.4*	0.1*
$(W_L'/W_{L0})_0$ (10^{-11} Pa^{-1})	30.05	11.26	8.06	2.1*	
$(W_S'/W_{S0})_0$ (10^{-11} Pa^{-1})	7.71	4.24	0.97	1.1*	
$(\partial C_L/\partial P)_{P=0}$	35.8	25.9	20	7.0*	24.1*
$(\partial \mu/\partial P)_{P=0}$	2.9	3.6	0.9	1.1	4.0*
$(\partial B^S/\partial P)_{P=0}$	31.9	21.0	18.8	5.5	18.8
γ^{el}	4.66	3.94	2.47		

postulated that some of the oxygen atoms in the Cu-O chain, when thermally stimulated in a certain temperature range, hop over to the next Cu-□ chain to fill the vacancies. Such a state is unstable and the atoms can then hop back to the Cu-O chain. Hence, a dynamic hopping process may take place in both Cu-O and Cu-□ chains. When $YBa_2Cu_3O_{6.6}$ is subjected to the strain field introduced by ultrasonic waves in the temperature region from 250 to 100 K, part of the sound energy is absorbed by the active oxygen atoms causing the attenuation peak.

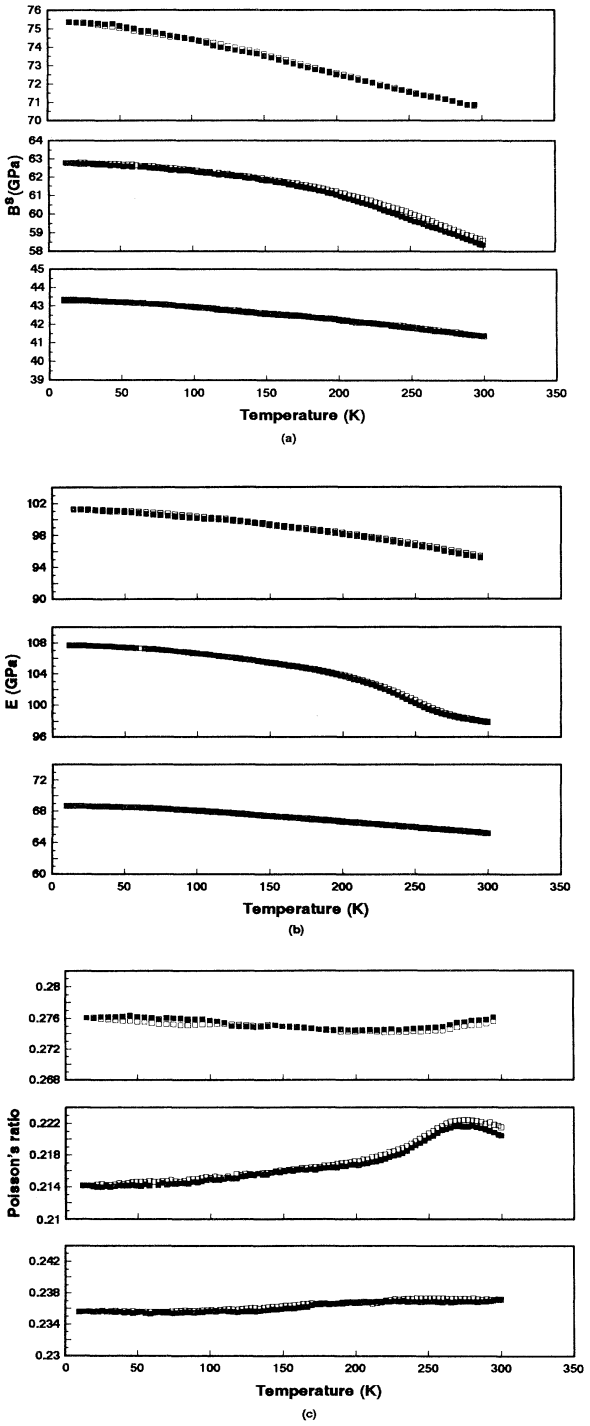

FIG. 5. Temperature dependence of (a) bulk modulus B^S, (b) Young's modulus E, and (c) Poisson's ratio σ of $YBa_2Cu_3O_{6.3}$ (bottom panel), $YBa_2Cu_3O_{6.6}$ (middle panel), and $YBa_2Cu_3O_{6.94}$ (upper panel). The solid (open) symbols correspond to data obtained during cooling (warming).

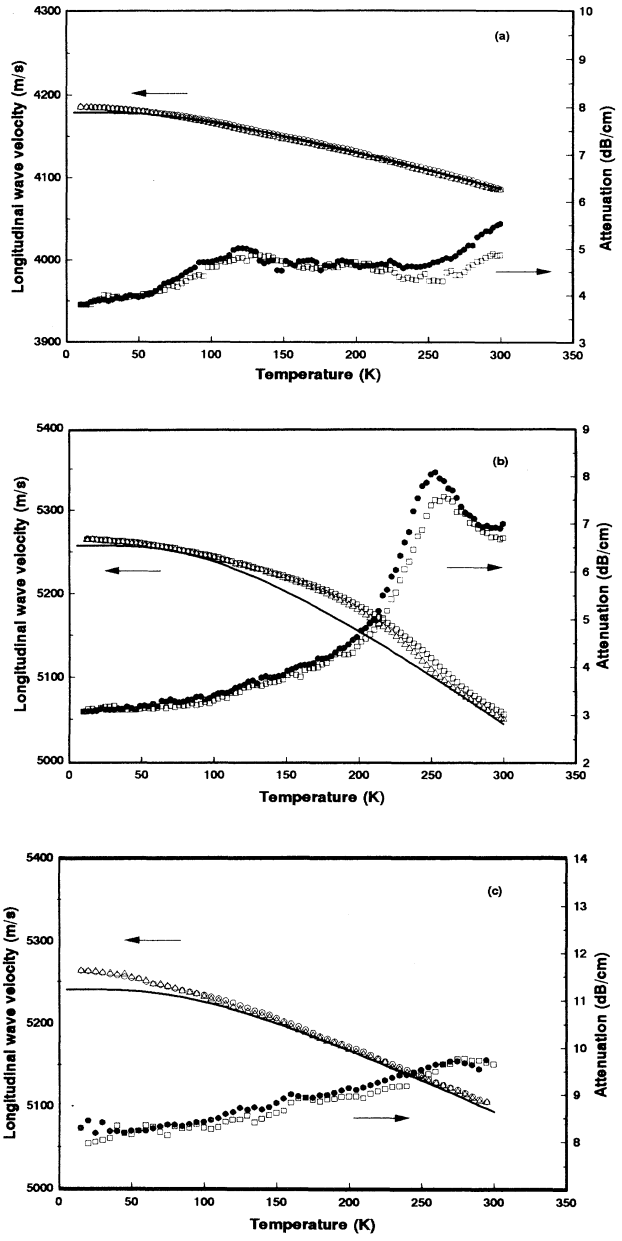

FIG. 6. Temperature dependence of longitudinal mode velocity (corrected for effects of porosity) and attenuation for (a) $YBa_2Cu_3O_{6.3}$, (b) $YBa_2Cu_3O_{6.6}$, and (c) $YBa_2Cu_3O_{6.94}$. The open circles in (a) and (c) are for the velocity during cooling. The open triangles are for the velocity during warming. The solid circles are for the attenuation during cooling. The open squares are for the attenuation during warming in (a)–(c) and the velocity during cooling in (c). The solid line is a fitting of Lakkad's phenomenological model [Eq. (1)] to the velocity versus temperature curves.

The energy absorption process depends on temperature. In this temperature range, the number of oxygen atoms hopping to the Cu-□ chains is larger than the number hopping back. The filling of vacant sites in the Cu-□ chains leads to the formation of instantaneously localized regions of ortho-I phase in $YBa_2Cu_3O_{6.6}$; these stiffen the material and cause the ultrasonic wave velocity to increase sharply. With further decrease in temperature, the thermally activated process ceases gradually and the material returns to the state dominated by the anharmonicity of atomic oscillators.

IV. EFFECTS OF HYDROSTATIC PRESSURE

The effects of hydrostatic pressure on the elastic properties of high-T_c superconductor $YBa_2Cu_3O_{7-x}$ can be investigated by determining the initial slope $(f')_0$ of the pulse-echo overlap frequency f versus pressure P curves obtained in the ultrasonic measurements. The advantage of using the natural velocity W is that the pressure derivative $[\partial(\rho_0 W^2)/\partial P]_{P=0}$ is directly related to $(f')_0$ by

$$\left.\frac{\partial(\rho_0 W^2)}{\partial P}\right|_{P=0} = 2\rho_0 v_0^2 \frac{(W')_0}{W_0} = 2\rho_0 v_0^2 \frac{(f')_0}{f_0} , \tag{3}$$

where ρ_0 and v_0 are the density and ultrasonic wave velocity at atmospheric pressure, respectively, $(W')_0$ is the initial hydrostatic pressure derivative of W, and f_0 is the intercept of the frequency versus pressure curve. The pressure derivatives of the longitudinal or shear modulus for isotropic materials can be calculated using[39]

$$\left[\frac{\partial M}{\partial P}\right]_{P=0} = \left[\frac{\partial(\rho_0 v_q^2)}{\partial P}\right]_{P=0} = \rho_0 v_{q0}^2 \left[\frac{2W_q'}{W_{q0}} + \frac{1}{3B^T}\right]_{P=0} , \tag{4}$$

where M is the longitudinal or shear modulus, the subscript q indicates the wave mode (L for longitudinal or S for shear), and B^T is the isothermal bulk modulus. The pressure derivatives $(\partial C_L/\partial P)_{P=0}$, $(\partial\mu/\partial P)_{P=0}$, and $(\partial B^S/\partial P)_{P=0}$ determined for the longitudinal modulus C_L, shear modulus μ, and the bulk modulus B^S for sintered ceramic samples $YBa_2Cu_3O_{6.3}$, $YBa_2Cu_3O_{6.6}$, and $YBa_2Cu_3O_{6.94}$ are given in Table IV, together with data reported by other authors for $YBa_2Cu_3O_{7-x}$. The hydrostatic pressure derivatives $(W_q'/W_{q0})_0$ of the natural velocities for both longitudinal and shear modes, the density ρ, and the porosity n of the ceramic samples are also given in Table IV for comparison.

A. The effects of porosity and cracking on the hydrostatic pressure derivatives of the elastic moduli

The values of the hydrostatic pressure derivatives of the elastic moduli of the three sintered ceramic samples (with the exception of that for the shear modulus) decrease in the order of $YBa_2Cu_3O_{6.3}$, $YBa_2Cu_3O_{6.6}$, and $YBa_2Cu_3O_{6.94}$, i.e., with increasing oxygen content (see Table IV). The relatively higher value of $(\partial\mu/\partial P)_{P=0}$ for $YBa_2Cu_3O_{6.6}$ is, in part, due to the higher value of the shear modulus μ for this compound. The porosity of the $YBa_2Cu_3O_{6.3}$ sample used for the ultrasonic measurements under pressure is large ($n=0.28$), which leads to a smaller value of μ ($=17.8$ GPa). This value, when substituted into Eq. (4), leads to a lower value of $(\partial\mu/\partial P)_{P=0}$.

The elastic modulus measured at atmospheric pressure enters explicitly into the calculation of $(\partial M/\partial P)_{P=0}$ [see Eq. (4)]. In order to avoid the complications associated with this, it is desirable to base the discussion on the pressure derivative $(W_q'/W_{q0})_0$ of the natural velocity W_q, which gives the pressure derivative of the velocity of the relevant mode. Table IV shows that, for $YBa_2Cu_3O_{6.3}$, the value of $(W_S'/W_{S0})_0$ for the shear mode is much larger than that for $YBa_2Cu_3O_{6.6}$, although the situation for the values of $(\partial\mu/\partial P)_{P=0}$ is the opposite. The decreasing trend of the hydrostatic pressure derivatives of the natural velocities for both modes is probably mainly caused by pores (or cracks) in the samples because the porosities of the samples also decrease in the order of $YBa_2Cu_3O_{6.3}$, $YBa_2Cu_3O_{6.6}$, and $YBa_2Cu_3O_{6.94}$ (Table IV).

Recently, Rigden, White, and Vance[40] measured the ultrasonic wave velocities of a hot-pressed sample of $YBa_2Cu_3O_{7-x}$, with a porosity of 0.06, up to 3 GPa. Their results show a nonlinearity in the pressure dependences of both longitudinal and shear velocities with progressively decreasing slopes. In the pressure range 1–3 GPa, they found values of 5.5 and 1.1 for $(\partial B^S/\partial P)$ and $(\partial\mu/\partial P)$, respectively, for this hot-pressed sample. Using

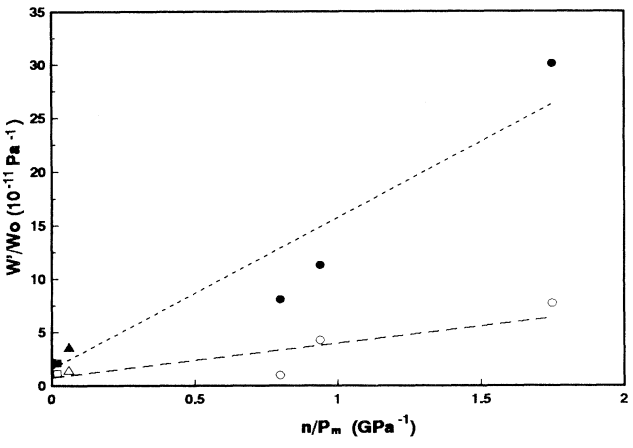

FIG. 7. Hydrostatic pressure derivatives $(W_L'/W_{L0})_0$ (solid symbols) and $(W_S'/W_{S0})_0$ (open symbols) of natural velocities of longitudinal and shear waves propagated in $YBa_2Cu_3O_{7-x}$ as a function of ratio n/P_m of porosity n to upper pressure limit P_m of measurements. The circles correspond to results obtained in this work for sintered ceramic samples of $YBa_2Cu_3O_{6.3}$, $YBa_2Cu_3O_{6.6}$, and $YBa_2Cu_3O_{6.94}$; the squares correspond to results for hot-pressed $YBa_2Cu_3O_{7-x}$, with $P_m=3$ GPa (Ref. 40), and the triangles to results estimated from data of Rigden, White, and Vance (Ref. 40), with $P_m=1$ GPa. The lines are intended as a guide to the eye.

their data for hot-pressed $YBa_2Cu_3O_{7-x}$, the values of $(\partial C_L/\partial P)$ and (W_q'/W_q) (for both longitudinal and shear modes) have now been estimated (Table IV). Their result for $(\partial\mu/\partial P)$ of the hot-pressed $YBa_2Cu_3O_{7-x}$ sample is almost the same as that $(\partial\mu/\partial P)_{P=0}$ determined in this work for sintered $YBa_2Cu_3O_{6.94}$, but the values given by Rigden, White, and Vance[40] for $(\partial B^S/\partial P)$ and $(\partial C_L/\partial P)$ of hot-pressed $YBa_2Cu_3O_{7-x}$ are much smaller than those obtained for sintered samples of $YBa_2Cu_3O_{6.3}$, $YBa_2Cu_3O_{6.6}$, and $YBa_2Cu_3O_{6.94}$ in this work and for pure $YBa_2Cu_3O_{7-x}$ estimated by Xu.[41] From a linear fit to their data up to 1 GPa, we find that the values of $(\partial C_L/\partial P)$, $(\partial B^S/\partial P)$, and $(\partial\mu/\partial P)$ increase by 1.4 (20%), 1.2 (22%), and 0.15 (14%), respectively, compared with those obtained from the data in the pressure range 1–3 GPa. Even if these increments are considered, the values of $(\partial C_L/\partial P)$ and $(\partial B^S/\partial P)$ are still much smaller than those obtained for $(\partial C_L/\partial P)_{P=0}$ and $(\partial B^S/\partial P)_{P=0}$ in this work and that by Xu.[41] A likely source for high values of $(\partial C_L/\partial P)_{P=0}$ and $(\partial B^S/\partial P)_{P=0}$ is that in the pressure range well below 1 GPa, sintered $YBa_2Cu_3O_{7-x}$ behaves as a soft material because of pores or cracks in the samples, as suggested by Holcomb and Mayo[42] and Rigden, White, and Vance.[40] Application of hydrostatic pressure causes the pores and cracks to close together, which results in prominent changes in the sample volume and hence in C_L and B^S. The effects of pores and cracks on the pressure dependences of elastic moduli can be neglected once the pressure exceeds about 1 GPa, when the narrow microcracks should be closed and consequently their contribution to pressure-induced volume change is minimal. In an investigation of the effect of microcracking on the elastic moduli of subsequently oxygenated, hot-pressed $YBa_2Cu_3O_{7-x}$ (with $T_c=91$ K and porosity $n=0.06$), Holcomb and Mayo[42] measured the ultrasonic wave velocities of shear modes up to 0.2 GPa and those of longitudinal modes up to 1 GPa. Estimations using their data show that the pressure derivative of the ultrasonic wave velocity is strongly pressure dependent. Holcomb and Mayo[42] observed that during the oxygenation process of the hot-pressed $YBa_2Cu_3O_{7-x}$, numerous microcracks were formed; the size of the microcracks was up to the order of micrometer. They suggested that the large pressure dependence of ultrasonic wave velocities and the bulk modulus is due to closing of narrow microcracks under pressure. Based on this proposition, Rigden, White, and Vance[40] argue that the anomalously large values of $(\partial B^S/\partial P)_{P=0}$, found for the coarse-grained[14,43] and very dense[44] $YBa_2Cu_3O_{7-x}$, can also be explained by the microcracking mechanism.

The combined effects of sample porosity and application of hydrostatic pressure on the ultrasonic wave velocities and bulk modulus of a ceramic material can be quantitatively characterized by the ratio n/P_m of porosity n to the upper pressure limit P_m of the measurements. The hydrostatic pressure derivatives $(W_q'/W_{q0})_0$ and $(\partial B^S/\partial P)_{P=0}$ obtained in this work, those estimated from the results of Rigden, White, and Vance,[40] and $(\partial B^S/\partial P)$ determined by Rigden, White, and Vance[40] between 1 and 3 GPa are plotted in Figs. 7 and 8 as a function of the ratio n/P_m. These figures show the increase with n/P_m of the hydrostatic pressure derivatives $(W_q'/W_{q0})_0$ of the natural velocities for both longitudinal

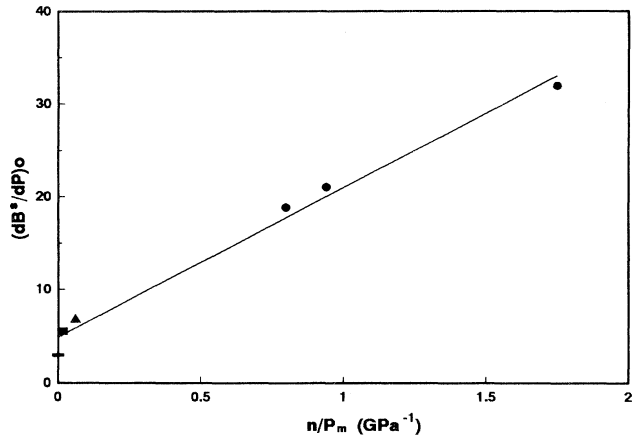

FIG. 8. Pressure derivative $(\partial B^S/\partial P)$ of $YBa_2Cu_3O_{7-x}$ as a function of ratio n/P_m of porosity n to upper pressure limit P_m of measurements. The solid circles correspond to $(\partial B^S/\partial P)_{P=0}$ obtained in this work for sintered ceramic samples of $YBa_2Cu_3O_{6.3}$, $YBa_2Cu_3O_{6.6}$, and $YBa_2Cu_3O_{6.94}$. The solid square corresponds to $(\partial B^S/\partial P)$ for hot-pressed $YBa_2Cu_3O_{7-x}$, with $P=1-3$ GPa (Ref. 40) and the solid triangle corresponds to $(\partial B^S/\partial P)_{P=0}$ estimated from data of Rigden, White and Vance (Ref. 40), with $P_m=1$ GPa. The bar is $(\partial B^T/\partial P)_{P=0}$ given by Olsen *et al.* (Ref. 45). The solid line is a least-squares fit to all of the above data [see Eq. (5)].

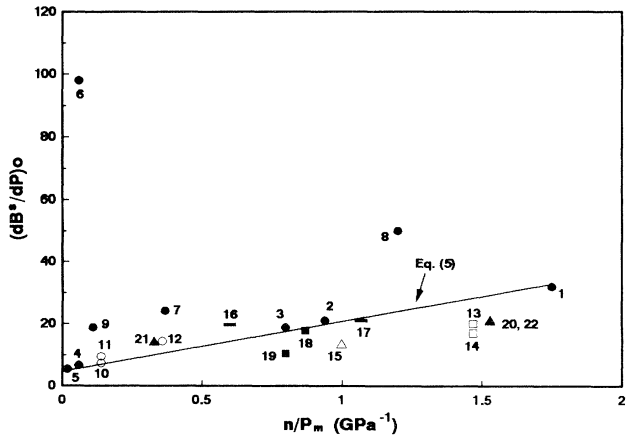

FIG. 9. Hydrostatic pressure derivative $(\partial B^S/\partial P)_{P=0}$ of bulk modulus of various high-T_c superconducting ceramics and some related nonsuperconducting compounds [including $(\partial B^S/\partial P)$ for hot-pressed $YBa_2Cu_3O_{7-x}$, with $P=1-3$ GPa (Ref. 40)], which were obtained from high-pressure ultrasonic studies, as a function of ratio n/P_m of porosity n to upper pressure limit P_m of measurements. Solid circles, $YBa_2Cu_3O_{7-x}$; open circles, $YBa_2Cu_3O_{7-x}$/Ag; open squares, $GdBa_2Cu_3O_{7-x}$; open triangle, $YBa_2Cu_4O_8$; bar La_2CuO_4 and $La_{1.8}Sr_{0.2}CuO_4$; solid squares, Nd_2CuO_{4+y} and $Nd_{1.85}Ce_{0.15}CuO_{4+y}$; and solid triangles, $Bi_2Sr_2CaCu_2O_{8+x}$ and $Bi_2Sr_2Ca_2Cu_3O_{10+x}$. Solid line represents Eq. (5). Labels indicate the sources of the data. For details and references, see Table V.

and shear modes [except $(W_S'/W_{S0})_0$ for $YBa_2Cu_3O_{6.94}$] and that of the pressure derivative $(\partial B^S/\partial P)_{P=0}$ of the bulk modulus. From high-pressure X-ray-diffraction measurements of the lattice parameters of $RBa_2Cu_3O_{7-x}$ (R =Y, Eu, and Ho) up to 60 GPa, Olsen *et al.*[45] obtained $(\partial B^T/\partial P)_0=2.9$ for $YBa_2Cu_3O_{7-x}$ by fitting the Murnaghan equation of state to the experimental data points. If this is taken as the "correct" value for the pressure derivative of the bulk modulus of $YBa_2Cu_3O_{7-x}$, free from pores and cracks, i.e., for $n/P_m=0$, a linear relationship can be found between $(\partial B/\partial P)$ and n/P_m for $P_m \leq 3$ GPa, i.e.,

$$\left[\frac{\partial B}{\partial P}\right]=4.94+16\frac{n}{P_m} . \quad (5)$$

This empirical relationship illustrates that the effects of pressure on the bulk modulus are more pronounced for samples with high porosity and subjected to a lower upper limit of applied hydrostatic pressure. To test Eq. (5), data obtained from high-pressure ultrasonic experiments for the pressure derivative $(\partial B^S/\partial P)_{P=0}$ of the bulk modulus of high-T_c superconducting ceramics, and some related nonsuperconducting compounds, have been compiled from a number of sources and plotted in Fig. 9. The source details and the related references are summarized in Table V. The solid straight line in Fig. 9 represents Eq. (5); it is the same as that shown in Fig. 8. It is clear that most of the experimental data points for various ceramics fall near this straight line, which corresponds to the results obtained in this work for sintered ceramic specimens of $YBa_2Cu_3O_{6.3}$, $YBa_2Cu_3O_{6.6}$, and $YBa_2Cu_3O_{6.94}$ and those for the hot-pressed $YBa_2Cu_3O_{7-x}$ by Rigden, White, and Vance.[40] This supports the analysis by which Eq. (5) has been derived and provides a measure of the important role played by the ratio n/P_m (sample porosity to the maximum pressure of measurements) in determining the hydrostatic pressure derivative $(\partial B^S/\partial P)_{P=0}$ of the bulk modulus of high-T_c ceramics. It may be noted that the results obtained by Holcomb and Mayo[42] for the subsequently oxygenated, hot-pressed $YBa_2Cu_3O_{7-x}$ are exceptionally large and deviate markedly from the trend found for other high-T_c ceramics (Fig. 9, labeled 6).

B. The effects of porosity on the Grüneisen parameters

Another important parameter related with high-pressure properties of materials, such as the bulk modulus and the pressure derivatives of the elastic modu-

TABLE V. Hydrostatic pressure derivative $(\partial B^S/\partial P)_{P=0}$ of the bulk modulus of various high-T_c superconducting ceramics and some related nonsuperconducting compounds obtained from high-pressure ultrasonic studies. n and P_m (in GPa) are sample porosity and maximum pressure applied in the measurements, respectively. "Label" is that of data points in Fig. 9. Coarse-grained $YBa_2Cu_3O_{7-x}$ (sample Y2) (Ref. 43) was the only specimen that showed pronounced hysteresis effects in pressure dependence of velocities of both longitudinal and shear ultrasonic waves. From a reanalysis of data obtained during increasing pressure, we have obtained a value of 24 for $(\partial B^S/\partial P)_{P=0}$ for this sample. * denotes $(\partial B^S/\partial P)$ for $P=1$–3 GPa.

Material	n	P_m	n/P_m	$\left[\frac{\partial B}{\partial P}\right]_{P=0}$	Ref.	Label
$YBa_2Cu_3O_{6.3}$	0.28	0.16	1.75	31.9	This work	1
$YBa_2Cu_3O_{6.6}$	0.15	0.16	0.94	21.0	This work	2
$YBa_2Cu_3O_{6.94}$	0.12	0.15	0.8	18.8	This work	3
$YBa_2Cu_3O_{7-x}$ (hot-pressed)	0.06	1.0	0.06	6.7	Estimated from Ref. 40	4
$YBa_2Cu_3O_{7-x}$ (hot-pressed)	0.06	3.0	0.02	5.5*	40	5
$YBa_2Cu_3O_{7-x}$ (hot-pressed, subsequently oxygenated)	0.06	1.0	0.06	98	42	6
$YBa_2Cu_3O_{7-x}$ (coarse-grained, increasing pressure)	0.056	0.15	0.37	24	Estimated from Ref. 43	7
$YBa_2Cu_3O_{7-x}$ (small-grained)	0.18	0.15	1.2	50	43	8
$YBa_2Cu_3O_{7-x}$	0.055	0.5	0.11	18.8	41	9
$YBa_2Cu_3O_{7-x}$/Ag (75 wt. %)	0.055	0.4	0.14	7.35	46	10
$YBa_2Cu_3O_{7-x}$/Ag (50 wt. %)	0.055	0.4	0.14	9.48	46	11
$YBa_2Cu_3O_{7-x}$/Ag (15 vol %)	0.054	0.15	0.36	14.3	47	12
$GdBa_2Cu_3O_{7-x}$ orthorhombic	0.22	0.15	1.47	20	48	13
$GdBa_2Cu_3O_{7-x}$ tetragonal	0.22	0.15	1.47	17	48	14
$YBa_2Cu_4O_8$	0.15	0.15	1.0	13.1	49	15
La_2CuO_4	0.09	0.15	0.6	19.7	50	16
$La_{1.8}Sr_{0.2}CuO_4$	0.16	0.15	1.07	21	50	17
Nd_2CuO_{4+y}	0.13	0.15	0.87	17.8	50	18
$Nd_{1.85}Ce_{0.15}CuO_{4-y}$	0.12	0.15	0.8	10.4	50	19
Bi2212 sintered	0.23	0.15	1.53	20.6	51	20
Bi2212 dense, textured	0.05	0.15	0.33	13.9	52	21
Bi2223 sintered	0.23	0.15	1.53	20.9	51	22

li, is the Grüneisen parameter. It is a dominant term in the theoretical evaluation of the pressure derivative of T_c in the BCS theory and it plays a significant role in studies of the contribution of the lattice vibrations to both the superconducting and normal properties of the superconductors.[53] The thermal Grüneisen parameter γ^{th} is related to the volume thermal expansion coefficient β, the specific heat C_P, the volume V, and the bulk modulus B^S by the equation

$$\gamma^{\text{th}}=\frac{\beta B^S V}{C_P} . \tag{6}$$

The mean acoustic-mode Grüneisen parameter γ^{el} accounts for the contribution of the overall long-wavelength acoustic modes to thermal expansion and can be evaluated from the bulk modulus and the pressure derivatives of the elastic moduli, using the equation

$$\gamma^{\text{el}}=\tfrac{1}{3}(\gamma_l+2\gamma_s) , \tag{7}$$

where

$$\gamma_l=\frac{-1}{6C_L}\left[C_L-3B^T\left[\frac{\partial C_L}{\partial P}\right]_{P=0}\right] \tag{8}$$

and

$$\gamma_s=\frac{-1}{6\mu}\left[\mu-3B^T\left[\frac{\partial \mu}{\partial P}\right]_{P=0}\right] . \tag{9}$$

Here γ_l and γ_s are the longitudinal and shear acoustic-mode Grüneisen parameters, respectively, and B^T is the isothermal bulk modulus which is little different from the adiabatic bulk modulus B^S and, as an approximation, can be replaced by B^S.

Normally γ^{th} is in the range from 1 to 3 for most solids. For some high-T_c materials the values of γ^{th} calculated by White,[54] using Eq. (6) with chosen B^S and "average" values of β and C_P, also fall in this range. However, for certain polycrystalline high-temperature superconductors the values of the mean acoustic-mode Grüneisen parameter γ^{el} determined by ultrasonic techniques spread over a wide range from 1.5 to 23.7.[43,44,47,49–52] The particular high values of γ^{el} were found for the coarse-grained and for the very dense ceramic samples of $YBa_2Cu_3O_{7-x}$.[43,44] Equations (7)–(9) indicate that the anomalous values found for the high-T_c polycrystalline materials may be caused by the large pressure derivatives of the elastic moduli measured for these materials, which, as indicated in the last section, are caused by the pores and cracks in those samples. Substitution from the data in Table IV into Eqs. (7)–(9) gives the values of γ^{el} for $YBa_2Cu_3O_{6.3}$, $YBa_2Cu_3O_{6.6}$, and $YBa_2Cu_3O_{6.94}$ compounds measured in this work as shown in Table IV. It is worth noting that the value of γ^{el} (2.47) for the $YBa_2Cu_3O_{6.94}$ compound is close to an "average" value (2.3) suggested by White[54] for the thermal Grüneisen parameter γ^{th} for $YBa_2Cu_3O_{7-x}$ at 295 K. From x-ray measurement of lattice parameters up to 1 GPa, Gavarri and Carel[55] determined $\gamma^{\text{th}}=2.7$ for $YBa_2Cu_3O_{7-x}$ at 300 K. To get a view of the effects of pores and cracks on the mean acoustic Grüneisen parameter γ^{el}, a linear regression has been made for γ^{el} of $YBa_2Cu_3O_{6.3}$, $YBa_2Cu_3O_{6.6}$, and $YBa_2Cu_3O_{6.94}$ compounds as a function of the porosity n,

$$\gamma^{\text{el}}=1.63+11.25n . \tag{10}$$

It gives a value of 1.63 to γ^{el} for void-free ($n=0$) $YBa_2Cu_3O_{7-x}$. This value is lower than that (2.3) suggested by White[54] for γ^{th}, but is very close to that (1.75) estimated by Schilling and Klotz[56] for γ^{th}. Schilling and Klotz[56] suggested that for high-T_c superconductors a value of γ^{th} between 1.5 and 2 is appropriate. Ledbetter[57] proposed a value of 1.38 for γ^{th} of $YBa_2Cu_3O_{7-x}$. Rigden, White, and Vance[40] estimated $\gamma^{\text{th}}\approx 1.25$ for $YBa_2Cu_3O_{7-x}$, based on their value for B^S (96 GPa) determined by ultrasonic measurements. By using the pressure derivatives of the elastic moduli estimated from their results between 0 to 1 GPa, a value of 1.35 has been found for γ^{el} at room temperature. There is another type of the Grüneisen parameter that can be estimated by using the pressure derivative of the isothermal bulk modulus and Slater's equation,[58]

$$\gamma=\frac{-1}{6}+\frac{1}{2}\left[\frac{\partial B^T}{\partial P}\right]_T . \tag{11}$$

If the value (4.94) obtained in the last section for the pressure derivative $(\partial B^S/\partial P)_{P=0}$ of the adiabatic bulk modulus B^S of a void-free $YBa_2Cu_3O_{7-x}$ compound is introduced into this equation, a value of 2.3 is obtained for the Slater γ. However, this equation was obtained making the assumption that the Poisson ratio is independent of volume, which could cause an error in the estimation of γ. Also, the difference between the pressure derivatives $(\partial B^T/\partial P)_{P=0}$ and $(\partial B^S/\partial P)_{P=0}$ may need to be

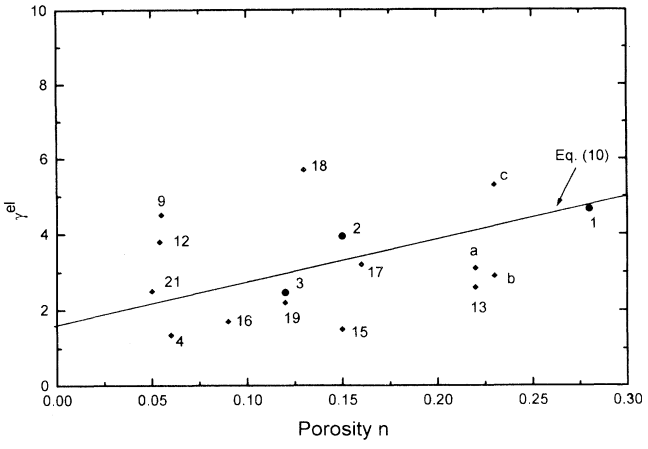

FIG. 10. The mean acoustic Grüneisen parameter γ^{el} of some high-T_c superconducting ceramics and some related nonsuperconducting compounds as a function of the porosity n. Solid line represents Eq. (10). Numbered labels indicate the sources of the data, as given in Table V. The labeled points *a*, *b*, and *c* are for $Bi_{1.8}Pb_{0.3}Sr_2Ca_2Cu_3O_{10}$ (sample 1), $Bi_{1.8}Pb_{0.3}Sr_2Ca_2Cu_3O_{10}$ (sample 2), and $Bi_{1.8}Pb_{0.3}Sr_2CaCu_8$, respectively (Ref. 51).

considered. It is clear from Eq. (10) that the change rate of γ^{el} with respect to the porosity n, $\partial\gamma^{el}/\partial n = 11.2$, is quite large: the effects of the porosity are significant. In order to check the fitted results of Eq. (10), the values of γ^{el} for some superconducting and related nonsuperconducting ceramics have been plotted, together with our results, in Fig. 10. It can be seen that Eq. (10) represents quite well the influence of the porosity n on γ^{el}. Hence, the result (1.63) obtained in Eq. (10) is suggested here as a reasonable value for the mean acoustic-mode Grüneisen parameter γ^{el} of void-free $YBa_2Cu_3O_{7-x}$ superconductors.

C. Effects of oxygen content on hydrostatic pressure derivatives of elastic moduli

In a structural study of copper-oxide superconductors, Loveday *et al.*[59] estimated the changes of bond lengths in $YBa_2Cu_3O_{7-x}$ under oxidation, by taking the average rate of change of the bond length with T_c. They found that the bond length Cu(2)-O(1) and the Ba-O(1) interlayer separations decrease, while the bond length Cu(1)-O(1) increases with increasing pressure. The changes in the bond lengths induced by the applied pressure are -2.1% for Cu(2)-O(1) under pressures up to 3.5 GPa and 1.1% for Cu(1)-O(1) up to 5 GPa. The change in the Ba-O(1) interlayer separation is -17.9% under pressures up to 5 GPa.[59] These changes resemble those induced in the bond lengths by varying oxygen content [see Fig. 2(a)–2(c)]. The pressure dependence of relative changes in the bond lengths Cu(2)-O(1) and Cu(1)-O(1) and in the Ba-O(1) interlayer separation have been calculated by using the data picked from the results of Loveday *et al.*[59] These relative changes are drawn in Figs. 2(a)–2(c) together with the data collected by Santoro[22] to show the correlation between applying pressure and changing the oxygen concentration. The increase of oxygen content can be thought of simplistically as applying a "chemical pressure" to the unit cell. Much of the largest change in bond length induced by the chemical pressure is that of Cu(2)-O(1) [see Fig. 2(a)]. The linear regression of the data in Fig. 3(a) for the dependence of the bulk modulus B^S of $YBa_2Cu_3O_{6+\delta}$ on δ shows that the oxygen content dependence $\partial B^S/\partial\delta$ is ≈ 64 GPa. In Table VI some collected data for the isothermal bulk modulus B^T, determined by x-ray- and neutron-diffraction studies of $YBa_2Cu_3O_{6+\delta}$, also show that the value of B^T increases with increasing oxygen contents. The linear regression of these data gives that $\partial B^T/\partial\delta \approx 36$ GPa, with $B^T \approx 99.2$ GPa for $YBa_2Cu_3O_6$ and $B^T = 134.9$ GPa for $YBa_2Cu_3O_7$. Hence, the chemical pressure dependence of the bulk modulus of the copper-oxide compound $YBa_2Cu_3O_{6+\delta}$ is large. Considering this sensitivity of the bulk modulus to oxygen content, it can be expected that the value of $(\partial B^S/\partial P)_{P=0}$ itself also depends on the oxygen content of $YBa_2Cu_3O_{6+\delta}$, or, in turn, that $(\partial B^S/\partial P)_{P=0}$ exhibits a chemical pressure dependence. Inspection of the results for $YBa_2Cu_3O_{7-x}$ presented in Table IV shows that the hydrostatic pressure derivatives $(\partial B^S/\partial P)_{P=0}$, $(\partial C_L/\partial P)_{P=0}$, $(W_L'/W_{L0})_0$, and $(W_S'/W_{S0})_0$ do decrease with reducing oxygen deficiency x. Although these values include the effects of microstructural defects (such as pores, cracks, grain boundary, and twinning) and it is difficult to separate the influence of the oxygen content, the influence of the oxygen content on these pressure derivatives still can be inferred from the data collected in Table IV. Linear regressions made on the results of $YBa_2Cu_3O_{6.3}$, $YBa_2Cu_3O_{6.6}$, and $YBa_2Cu_3O_{6.94}$ compounds and Xu's results[41] show that the change $\Delta(\partial B^S/\partial P)_{P=0}/\Delta\delta$ of the pressure derivative $(\partial B^S/\partial P)_{P=0}$ with increasing oxygen content δ is -19.6 ± 5.4, while that of $(\partial C_L/\partial P)_{P=0}$ is -21.4 ± 4.9. Within the range of the errors, the change of the pressure derivatives of the two volume-dependent moduli B^S and C_L with δ, as shown in Figs. 11(a) and 11(b), is similar: change in the volume induced by varying the oxygen content does lead to oxygen content dependences of the pressure derivatives $(\partial B^S/\partial P)_{P=0}$ and $(\partial C_L/\partial P)_{P=0}$. Unlike the volume-dependent properties of $(\partial B^S/\partial P)_{P=0}$ and $(\partial C_L/\partial P)_{P=0}$, the value of $(\partial\mu/\partial P)_{P=0}$ for the shear mode does not show a systematic dependence on the oxygen content but scatters in the range $\approx 1-4$ (Table IV). A recent review by Fietz *et al.*[63] illustrates that the oxygen content of $YBa_2Cu_3O_{7-x}$ has a pronounced effect on its elastic behavior under pressure: $(\partial B/\partial P)$ decreases with increasing oxygen content, a finding that agrees with the results of this work for $YBa_2Cu_3O_{6.3}$, $YBa_2Cu_3O_{6.6}$, and $YBa_2Cu_3O_{6.94}$ samples.

It can be seen in Table IV that the mean acoustic-mode Grüneisen parameter γ^{el} increases with increasing oxygen deficiency x. A linear regression shows that the rate of change of γ^{el} for $YBa_2Cu_3O_{6.3}$, $YBa_2Cu_3O_{6.6}$, and $YBa_2Cu_3O_{6.94}$ samples with respect to oxygen deficiency x is $\partial\gamma^{el}/\partial x \approx 3.4$. Although this value includes the effects of pores and cracks, it does show that there exists an influence of oxygen content on the lattice vibrational

TABLE VI. Collection of the values for the isothermal bulk modulus B^T of $YBa_2Cu_3O_{6+\delta}$, determined by x-ray and neutron diffraction, as a function of oxygen content δ.

$YBa_2Cu_3O_{6+\delta}$	B^T (GPa)	Reference	$YBa_2Cu_3O_{6+\delta}$	B^T (GPa)	Reference
$YBa_2Cu_3O_{6.00}$	110	60	$YBa_2Cu_3O_{6.78}$	115	60
$YBa_2Cu_3O_{6.2}$	115	61	$YBa_2Cu_3O_{6.8}$	126	61
$YBa_2Cu_3O_{6.4}$	112	62	$YBa_2Cu_3O_{6.86}$	118	60
$YBa_2Cu_3O_{6.60}$	112	60	$YBa_2Cu_3O_{6.9}$	175	62
$YBa_2Cu_3O_{6.6}$	112	19	$YBa_2Cu_3O_{6.93}$	123	19
$YBa_2Cu_3O_{6.7}$	128	61	$YBa_2Cu_3O_{6.95}$	130	61

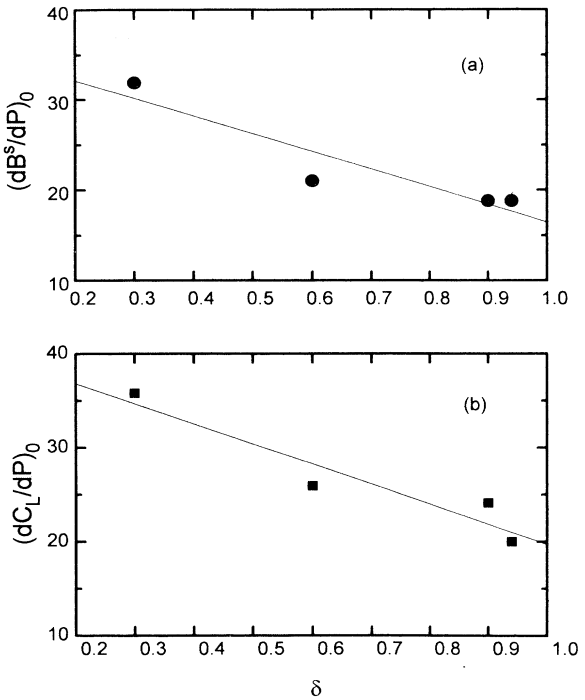

FIG. 11. Oxygen content (δ) dependence of pressure derivatives (a) $(\partial B^S/\partial P)_{P=0}$ and (b) $(\partial C_L/\partial P)_{P=0}$. Data are those determined in this work for $YBa_2Cu_3O_{6.3}$, $YBa_2Cu_3O_{6.6}$, and $YBa_2Cu_3O_{6.94}$ and those of Xu (Ref. 41) for $YBa_2Cu_3O_7$ (see Table IV).

anharmonicity of $YBa_2Cu_3O_{7-x}$. This should be related to the weakening of the interionic forces caused by a decrease in oxygen content with increasing x, as has been found in Sec. III B.

V. CONCLUSIONS

The temperature and hydrostatic pressure dependence of the ultrasonic wave velocities of sintered $YBa_2Cu_3O_{7-x}$ containing various contents of oxygen, $YBa_2Cu_3O_{6.3}$, $YBa_2Cu_3O_{6.6}$, and $YBa_2Cu_3O_{6.94}$, establish the following features:

(1) The longitudinal velocity and modulus, and the bulk and Young's moduli for the three $YBa_2Cu_3O_{7-x}$ ceramics increase with oxygen content. This systematic change would be expected to result from a volume-dependent mechanism. This volume-dependent mechanism, accounted for by using the structural data of $YBa_2Cu_3O_{7-x}$, is a weakening of the interionic forces caused by a decrease in oxygen content with increasing x.

(2) The temperature dependence of the elastic moduli of $YBa_2Cu_3O_{6.3}$ and $YBa_2Cu_3O_{6.94}$ can be fitted to the lattice vibrational anharmonicity model down to 40 and 100 K, respectively, but with different temperature rates. A sharp rise has been observed in the ultrasonic wave velocities and elastic moduli of $YBa_2Cu_3O_{6.6}$ with decreasing temperature from 270 to 200 K. The fitting of the phenomenological model to the elastic moduli versus temperature curves and examining the ultrasonic attenuation data have led us to the hypothesis that in this temperature range there is a relaxation process producing an enhancement of the elastic properties of $YBa_2Cu_3O_{6.6}$ by oxygen hopping within this compound.

(3) The hydrostatic pressure derivatives of the elastic moduli of the three specimens of polycrystalline $YBa_2Cu_3O_{7-x}$ with differing oxygen content have been determined from measurements of the effects of hydrostatic pressure on the natural velocities of ultrasonic waves propagated in the specimens. The volume-dependent properties $(\partial B^S/\partial P)_{P=0}$ and $(W_L'/W_{L0})_0$ tend to decrease with increasing oxygen content. Analysis of the results obtained in structural studies of the copper-oxide superconductor $YBa_2Cu_3O_{6+\delta}$ suggests that systematic changes in the $(\partial B^S/\partial P)_{P=0}$ and $(W_L'/W_{L0})_0$ of $YBa_2Cu_3O_{6.3}$, $YBa_2Cu_3O_{6.6}$, and $YBa_2Cu_3O_{6.94}$ are related to the chemical pressure introduced by increased oxygen content δ.

(4) A comparison of the results obtained by different methods of correcting for the effects of pores and cracks (assuming different shapes and sizes of cracks) on the ultrasonic wave velocities and the elastic moduli shows that the values of ultrasonic wave velocities and elastic moduli of ceramic $YBa_2Cu_3O_{7-x}$ are strongly dependent on sample porosity and on the aspect ratio of cracks. Porosity n is the main factor that affects the elastic properties of ceramics. Using the results for the pressure derivatives $(\partial B^S/\partial P)_{P=0}$ obtained in this work and given by Olsen *et al.*[45] and $(\partial B^S/\partial P)$ reported by Rigden, White, and Vance,[40] we have developed an empirical relationship between $(\partial B^S/\partial P)$ and the ratio n/P_m (of the sample porosity n to the maximum applied pressure P_m) when $P_m \leq 3$ GPa; $(\partial B^S/\partial P)$ increases linearly with increasing n/P_m. This indicates that the ratio n/P_m has a significant influence on the determination of the hydrostatic pressure derivative $(\partial B^S/\partial P)$, and therefore $(\partial B^S/\partial P)_{P=0}$, of the bulk modulus of high-T_c ceramics. This view is supported by the fact that most of the data collected from various sources for the pressure derivative $(\partial B^S/\partial P)_{P=0}$ of the bulk modulus of high-T_c superconducting ceramics, and some related nonsuperconducting compounds, correlate with the straight line described by this relation.

(5) The mean acoustic Grüneisen parameter γ^{el} of the three compounds has been calculated. The results show that the value of this parameter increases with the porosity n. A linear regression gives a value of 1.63 for γ^{el} of a void-free $YBa_2Cu_3O_{7-x}$ compound, which is close to the thermal Grüneisen parameter γ^{th} (1.75) calculated[56] by using the bulk modulus determined by neutron diffraction.[19] The collected values for some superconducting and related nonsuperconducting compounds justify that the linear regression of the results of this work represents the characteristics of the dependence of γ^{el} on the porosity n. The results of this work also show that the value of γ^{el} increases with oxygen deficiency x, i.e., the lattice vibrational anharmonicity increases, which is a result of the weakening of the interionic forces when O(4) is removed gradually.

ACKNOWLEDGMENTS

We are grateful to the Science and Engineering Research Council (SERC) for financial support. We would like to thank W. A. Lambson for polishing the samples and H. R. Perrott for the scanning electron microscopy. M.C. is also grateful to TUBITAK (Grant No. TBAG-1209) for partial support. The work at Argonne National Laboratory was supported by the U.S. Department of Energy (DOE), Energy Efficiency and Renewable Energy, as part of a DOE program to develop electric power technology, under Contract No. W-31-109-Eng-38.

[1]T. J. Kim, B. Lüthi, M. Schwarz, H. Kühnberger, B. Wolf, G. Hampel, D. Nikl, and W. Grill, J. Magn. Magn. Mater. **76** & **77**, 604 (1988).

[2]A. Hikata, M. J. McKenna, C. Elbaum, R. Kershaw, and A. Wold, Phys. Rev. B **40**, 5247 (1989).

[3]P. Lemmens, C. Honnekes, M. Brakmann, S. Ewert, A. Comberg, and H. Passing, Physica C **162-164**, 452 (1989).

[4]H. M. Ledbetter, J. Mater. Res. **7**, 2905 (1992).

[5]U. Balachandran, R. B. Poeppel, J. E. Emerson, S. A. Johnson, M. T. Lanagan, C. A. Youngdahl, K. C. Goretta, and N. G. Error, Mater. Lett. **8**, 454 (1989).

[6]H. M. O'Bryan and P. K. Gallagher, J. Mater. Res. **3**, 619 (1988).

[7]T. Furukawa, T. Shigematsu, and N. Nakanishi, Physica C **204**, (1992).

[8]E. P. Papadakis, J. Acoust. Soc. Am. **42**, 1045 (1967).

[9]E. Kittinger, Ultrasonics **15**, 30 (1977).

[10]R. N. Thurston and K. Brugger, Phys. Rev. **133**, A1604 (1964).

[11]M. Cankurtaran, G. A. Saunders, and K. C. Goretta, Supercond. Sci. Technol. **7**, 4 (1994).

[12]C. M. Sayers and R. L. Smith, Ultrasonics **20**, 201 (1982).

[13]P. Lloyd and M. V. Berry, Proc. Phys Soc. **91**, 678 (1967).

[14]M. Cankurtaran, G. A. Saunders, J. R. Willis, A. Al-Kheffaji, and D. P. Almond, Phys. Rev. B **39**, 2872 (1989).

[15]H. M. Ledbetter, M. W. Austin, S. A. Kim, and Ming Lei, J. Mater. Res. **2**, 786 (1987).

[16]H. M. Ledbetter and S. K. Datta, J. Acoust. Soc. Am. **79**, 239 (1986).

[17]B. Budiansky and R. J. O'Connell, Int. J. Solids Struct. **12**, 81 (1976).

[18]Y. Shindo, H. Ledbetter, and H. Nozaki, J. Mater. Res. **10**, 7 (1995).

[19]J. D. Jorgensen, Shiyou Pei, P. Lightfoot, D. G. Hinks, B. W. Veal, B. Dabrowski, A. P. Paulikas, R. Kleb, and I. D. Brown, Physica C **171**, 93 (1990).

[20]Y. Yan, Marie-Geneviève Blanchin, C. Picard, and P. Gerdanian, J. Mater. Chem. **3**, 603 (1993).

[21]D. de Fontaine, G. Ceder, and M. Asta, Nature **343**, 544 (1990).

[22]A. Santoro, in *High Temperature Superconductivity,* edited by J. W. Lynn (Springer-Verlag, New York, 1990), p. 84.

[23]P. Strobel, J. J. Capponi, C. Chailout, M. Marezio, and J. L. Tholence, Nature **327**, 306 (1987).

[24]F. Beech, S. Miraglia, A. Santoro, and R. S. Roth, Phys. Rev. B **35**, 8778 (1987).

[25]A. Santoro, S. Miraglia, F. Beech, S. A. Sunshine, D. W. Nurphy, L. F. Schneemeyer, and J. V. Waszczak, Mater. Res. Bull. **22**, 1007 (1987).

[26]W. I. F. David, W. T. A. Harrison, J. M. F. Gunn, O. Moze, A. K. Soper, P. Day, J. D. Jorgensen, D. G. Hinks, M. A. Beno, L. Soderholm, D. W. Capone II, I. K. Schuller, C. U. Segre, K. Zhang, and J. D. Grace, Nature **327**, 310 (1987).

[27]J. D. Jorgensen, B. W. Veal, A. P. Paulikas, L. J. Nowicki, G. W. Crabtree, H. Claus, and W. K. Kwok, Phys. Rev. B **41**, 1863 (1990).

[28]E. Drescher-Krasicka, in *Internal Friction and Ultrasonic Attenuation in Solids Including High-T_c Superconductors,* edited by L. B. Magalas and S. Gorczyca, Materials Science Forum, Vols. 119–121 (Trans Tech Publications, Switzerland, 1993), pp. 631–642.

[29]B. Golding, W. H. Haemmerle, L. F. Schneemeyer, and J. V. Waszczak, *1988 IEEE Ultrasonics Symposium Proceedings* (IEEE, Piscataway, NJ, 1988), p. 1079.

[30]M. Saint-Paul, J. L. Tholence, H. Noel, J. C. Levet, M. Potel, and P. Gougeon, Solid State Commun. **69**, 1161 (1989).

[31]S. C. Lakkad, J. Appl. Phys. **42**, 4277 (1971).

[32]He Yusheng, Zhang Baiwen, Lin Sihan, Xiang, Jiong, Lou Yongming, and Chen Haoning, J. Phys. F **17**, L243 (1987).

[33]Wang Yening, Shen Huiming, Zju Jinsong, Xu Ziran, Gu Min, Niu Zhongmin, and Zhang Zhifang, J. Phys. C **20**, L665 (1987).

[34]G. Cannelli, R. Cantelli, F. Cordero, G. A. Costa, M. Ferretti, and G. L. Olcese, Phys. Rev. B **36**, 8907 (1987).

[35]M.-F. Xu, H-P. Baum, A. Schenström, B. K. Sarma, M. Levy, K. J. Sun, L. E. Toth, S. A. Wolf, and D. U. Gubser, Phys. Rev. B **37**, 3675 (1988).

[36]T. Lagreid and K. Fossheim, Europhys. Lett. **6**, 725 (1988).

[37]G. Cannelli, R. Cantelli, and F. Cordero, Phys. Rev. B **38**, 7200 (1988).

[38]D. P. Almond, Qingxian Wang, J. Freestone, E. F. Lambson, B. Chapman, and G. A. Saunders, J. Phys. Condens. Matter **1**, 6853 (1989).

[39]R. N. Thurston, Proc. IEEE **53**, 1320 (1965).

[40]S. Ridgen, G. K. White, and E. R. Vance, Phys. Rev. B **47**, 1153 (1993).

[41]Ji-an Xu, Supercond. Sci. Technol. **7**, 1 (1994).

[42]D. J. Holcomb and M. J. Mayo, J. Mater. Res. **5**, 1827 (1990).

[43]A. Al-Kheffaji, M. Cankurtaran, G. A. Saunders, D. P. Almond, E. F. Lambson, and R. C. J. Draper, Philos. Mag. B **59**, 487 (1989).

[44]M. Cankurtaran, G. A. Saunders, K. C. Goretta, and R. B. Poeppel, Phys. Rev. B **46**, 1157 (1992).

[45]J. S. Olsen, S. Stenstrup, I. Johannsen, and L. Gerward, Z. Phys. B Condens. Matter **72**, 165 (1988).

[46]J. Xu, R. Wang, M. H. Manghnani, A. Misra, Y. Song, and J. R. Gaines, J. Appl. Phys. **70**, 7182 (1991).

[47]M. Cankurtaran and G. A. Saunders, Supercond. Sci. Technol. **5**, 210 (1992).

[48]M. Cankurtaran, A. Al-Kheffaji, G. A. Saunders, D. P. Almond, and J. Freestone, Supercond. Sci. Technol. **3**, 76 (1990).

[49]M. Cankurtaran, G. A. Saunders, U. Balachandran, R. B. Poeppel, and K. C. Goretta, Supercond. Sci. Technol. **6**, 75 (1993).

[50]Chang Fanggao, M. Cankurtaran, G. A. Saunders, A. Al-Kheffaji, D. P. Almond, P. J. Ford, and D. A. Ladds, Phys. Rev. B **43**, 5526 (1991).

[51]Chang Fanggao, M. Cankurtaran, G. A. Saunders, A. Al-Kheffaji, D. P. Almond, and P. J. Ford, Supercond. Sci. Technol. **4**, 13 (1991).

[52]G. A. Saunders, Chang Fanggao, Li Jiaqiang, Q. Wang, M. Cankurtaran, E. F. Lambson, P. J. Ford, and D. P. Almond, Phys. Rev. B **49**, 9862 (1994).

[53]H. J. Liu, Q. Wang, G. A. Saunders, D. P. Almond, B. Chapman, and K. Kitahama, Phys. Rev. B **51**, 9167 (1995).

[54]G. K. White, in *Studies of High Temperature Superconductors: Advances in Research and Applications,* edited by A. Narlikar (Nova Science, New York, 1992), Vol. 9, pp. 121–148.

[55]J. R. Gavarri and C. Carel, Physica C **166**, 323 (1990).

[56]J. S. Schilling and S. Klotz, in *Physical Properties of High Temperature Superconductors III,* edited by D. M. Ginsburg (World Scientific, Singapore, 1992), pp. 59–157.

[57]H. Ledbetter, Physica C **159**, 488 (1989).

[58]J. C. Slater, *Introduction to Chemical Physics* (McGraw-Hill, New York, 1939), p. 239.

[59]J. S. Loveday, R. J. Nelmes, M. I. McMahon, D. R. Allan, E. Kaldis, J. Karpinski, B. Raveau, and V. Caignaert, Ferroelectrics **128**, 93 (1992).

[60]I. V. Aleksandrov, A. F. Goncharov, and S. M. Stishov, JETP Lett. **47**, 428 (1988).

[61]I. V. Medvedeva, Yu. S. Bersenev, B. A. Gizhevsky, N. M. Chebotaev, S. V. Naumov, and G. B. Demishev, Z. Phys. B **81**, 311 (1990).

[62]V. P. Glazkov, I. N. Goncharenko, and V. A. Somenkov, Sov. Phys. Solid State **30**, 2127 (1988).

[63]W. H. Fietz, H. A. Ludwig, B. P. Wagner, K. Grube, R. Benischke, and H. Wühl, in *Proceedings of NATO ARW on Frontiers of High Pressure Research,* edited by H. D. Hochheimer and R. D. Etters (Plenum, New York, 1992), p. 433.